REPORT DOCUMENTATION PAGE

Form Approved OMB No. 0704-0188

1. REPORT DATE *(DD-MM-YYYY)*	2. REPORT TYPE	3. DATES COVERED *(From – To)*
22-05-2009	Final Report	1 September 2008 - 01-Mar-09

4. TITLE AND SUBTITLE

Damage tolerant strategies for composite damage detection and health monitoring

5a. CONTRACT NUMBER
FA8655-08-1-3053

5b. GRANT NUMBER

5c. PROGRAM ELEMENT NUMBER

6. AUTHOR(S)

Professor Constantinos Soutis

5d. PROJECT NUMBER

5d. TASK NUMBER

5e. WORK UNIT NUMBER

7. PERFORMING ORGANIZATION NAME(S) AND ADDRESS(ES)

The University of Sheffield
Faculty of Engineering (Aerospace)
Sheffield S1 3JD
United Kingdom

8. PERFORMING ORGANIZATION REPORT NUMBER

N/A

9. SPONSORING/MONITORING AGENCY NAME(S) AND ADDRESS(ES)

EOARD
Unit 4515 BOX 14
APO AE 09421

10. SPONSOR/MONITOR'S ACRONYM(S)

11. SPONSOR/MONITOR'S REPORT NUMBER(S)
Grant 08-3053

12. DISTRIBUTION/AVAILABILITY STATEMENT

Approved for public release; distribution is unlimited.

13. SUPPLEMENTARY NOTES

14. ABSTRACT

This report results from a contract tasking The University of Sheffield as follows: The proposed exploratory work will focus on the following 4 interconnected areas and related issues:
The development of highly sensitive techniques for detecting and characterizing various types of damage in a composite material utilizing minimally invasive, non intrusive, permanently attached sensors and actuators, which is an open issue and should be first addressed.
The question how reliable and effective is a given SHM system to detect and characterize damage?should be formally and qualitatively predicted.
The question how serious is the effect of detected damage on the performance and integrity of the monitored structure?should be quantitatively answered.
Finally, the issue of possible actions required for proper damage mitigation and remedy has to be addressed.

15. SUBJECT TERMS
EOARD, Damage Tolerance, Structures, Composites

16. SECURITY CLASSIFICATION OF:			17. LIMITATION OF ABSTRACT	18, NUMBER OF PAGES	19a. NAME OF RESPONSIBLE PERSON
a. REPORT	b. ABSTRACT	c. THIS PAGE			SURYA SURAMPUDI
UNCLAS	UNCLAS	UNCLAS	UL	25	19b. TELEPHONE NUMBER *(Include area code)* +44 (0)1895 616021

FINAL REPORT

EOARD EXPLORATORY GRANT (FA8655-08-1-3053):

Preliminary Studies on Damage Tolerant Strategies for Composite Design and Health Monitoring

By the
The University of Sheffield (UK) and The University of Patras (GR)

Principal Investigator (s):
Costas Soutis, Professor and Head of Aerospace Engineering
Faculty of Engineering (Aerospace)
Mappin Street
Sheffield S1 3JD
Tel: +44-114-2227811, +44-114-2227837 (secretary)
Fax: +44-114-2227836
E-mail: c.soutis@sheffield.ac.uk

Dimitris Saravanos, Professor
Department of Mechanical Engineering and Aeronautics
Structural Analysis and Smart Materials Group
University of Patras, Patras, GR 265000, Greece
tel: +30-2610-969437, +30-2610-997233(Lab Secretary)
fax: +30-2610-992644
e-mail: saravanos@mech.upatras.gr

Table of Contents

This final report describes the work progress and other relevant actions performed during the last six months of this EOARD funded project.

1. EXPLORATORY RESEARCH WORK

TASK 1: Distributed Sensing and Actuation for SHM in Composite Materials

The scope of this task was to investigate the current state of art in distributed sensors and actuators and SHM techniques [1-4], with potential to be used in the detection of common and critical damage in composite materials.

COMPOSITE DAMAGE

Based on a conducted literature survey and previous experience of the University of Sheffield (UoS) group [5-8], three critical types of damage and propagation mechanisms were identified in laminated composite materials, subject to static, thermal or fatigue loading, Figure 1. These are: **matrix cracks** in cross- or angle-plies of the laminate, which subsequently bridge across the ply thickness; (2) **delamination cracks** at the ply interfaces developed either near the free-edges or initiated by the bridging or transverse matrix cracks; and (3) a combination of transverse and delamination and bridged matrix cracks, termed as **H cracks**. These types of damage remain invisible, and have an effect on the residual stiffness and strength of a composite structure. Their on-line detection and localization through suitable SHM strategy, and the evaluation of their effect on the residual stiffness and strength of the composite structure will be of paramount importance towards the development of the proposed damage tolerant strategies.

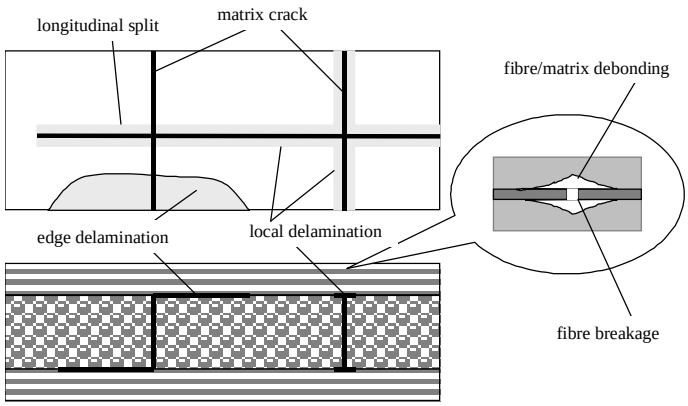

Figure 1. Damage mechanisms in composite laminates under tension-tension fatigue [6]

Damage Characterization

Figure 2 shows a cross-ply $[0_m/90_n]_s$ laminate subjected to biaxial tension ($\bar{s}_{11}$ and $\bar{s}_{22}$) and shear loading ($\bar{s}_{12}$). Suppose transverse and longitudinal matrix cracks are spaced uniformly and span the full thickness and width of the 90^o and 0^o plies respectively, and strip-shaped transverse and longitudinal delaminations grow along respective sets of cracks at the $0^o/90^o$ interface. Let $2s_1$ and $2s_2$ denote the spacing between longitudinal and transverse cracks, and $2\lambda_1$ and $2\lambda_2$ denote the width of longitudinal and transverse delamination strips, respectively.

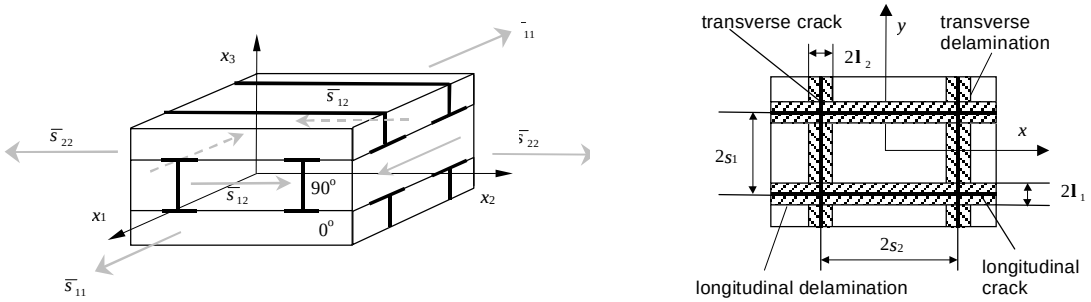

a) b)

Figure 2. Damaged cross-ply laminate under general in-plane loading: a) general view; b) plan view

Equivalent Constraint Model (ECM)

To analyze cracks associated with delaminations, it was suggested [2] to consider the following two ECM laminates instead of a representative segment the damaged laminate defined by intersecting pairs of cracks. In the ECM1 laminate, the 0^o layer (1^{st} layer) contains damage explicitly, while the 90^o layer (2^{nd} layer), damaged by transverse cracking and transverse delaminations, is replaced with a homogeneous equivalent constraint one with reduced stiffness properties. Likewise, in the ECM2 laminate, the 90^o layer (2^{nd} layer) is damaged explicitly, while the 0^o layer (1^{st} layer), damaged by longitudinal matrix cracks and longitudinal delaminations, is replaced with a homogeneous equivalent constrained layer with reduced stiffness properties.

The purpose of the analysis of the ECM1 laminate is to determine the stress field in its explicitly damaged 1^{st} layer and the reduced stiffness properties of the homogeneous equivalent layer. It is assumed that the stiffness properties of the equivalent constraint 2^{nd} layer, used in the analysis of the ECM1 laminate, are known from the analysis of the ECM2 laminate. This makes the problems for the analysis of the ECM1 and ECM2 laminates entwined.

Stress Analysis

ECM1 and ECM2 laminates are referred to the co-ordinate system $x_1x_2x_3$ (Fig. 2). A representative segment of an ECMm laminate, containing either a pair of cracks ($m=1$) or a single crack ($m=2$) and two crack tip delaminations, can be segregated into the locally

delaminated ($0 <| x_m |< \mathbf{l}_m$) and perfectly bonded ($\mathbf{l}_m <| x_m |< s_m$) regions. Due to symmetry, the analysis can be restricted to one quarter of the segment (Fig. 3).

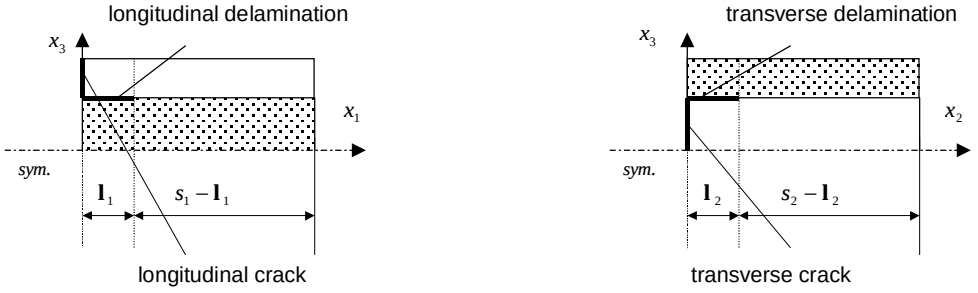

a) b)

Figure 3. Representative through-thickness segments of: a) ECM1 laminate; b) ECM2 laminate.

Since crack and delamination surfaces are assumed stress-free, stresses in the locally delaminated region of the explicitly damaged m^{th} ply vanish. In the perfectly bonded region, the in-plane microstresses $s_{jm}^{(m,m)}$, $j = 1,2$ can be determined from the equilibrium equations

$$\frac{d}{dx_m}\tilde{s}_{jm}^{(m,m)} + (-1)^m \frac{t_j^{(m)}}{h_m} = 0, \quad j,m = 1,2 \tag{1}$$

The out-of-plane shear stresses are assumed to vary linearly across the thickness of the 90^o layer as well as over one-single-ply thickness in the 0^o layer (so called shear layer) [21]. By integrating the constitutive equations for the out-of-plane shear stresses (see Appendix A of [22]), the interface shear stresses $t_j^{(m)}$ are expressed as

$$t_j^{(m)} = K_j(\tilde{u}_j^{(m,1)} - \tilde{u}_j^{(m,2)}), \quad K_j = \frac{3\hat{G}_{j3}^{(1)}\hat{G}_{j3}^{(2)}}{h_2\hat{G}_{j3}^{(1)} + (1+(1-h)/2)hh_1\hat{G}_{j3}^{(2)}}, \quad h = t/h_1 \tag{2}$$

Substitution of shear lag equations, Eqs. (2), into equilibrium equations, Eqs. (1) and subsequent differentiation with respect to x_m yield

$$\frac{d^2}{dx_m^2}\tilde{s}_{mm}^{(m,m)} + (-1)^m \frac{K_j}{h_m}(\tilde{e}_{mm}^{(m,1)} - \tilde{e}_{mm}^{(m,2)}) = 0, \quad \frac{d^2}{dx_m^2}\tilde{s}_{12}^{(m,m)} + (-1)^m \frac{K_j}{h_m}(\tilde{g}_{12}^{(m,1)} - \tilde{g}_{12}^{(m,2)}) = 0 \tag{3}$$

Strain differences $(\tilde{e}_{mm}^{(m,1)} - \tilde{e}_{mm}^{(m,2)})$ and $(\tilde{g}_{12}^{(m,1)} - \tilde{g}_{12}^{(m,2)})$ can be expressed in terms of stresses $\tilde{s}_{mm}^{(m,m)}$ and $\tilde{s}_{12}^{(m,m)}$, using the equations of the global equilibrium of the laminate, constitutive equations for both layers, as well as the condition of generalised plane strain in the plane $Ox_m x_3$. Finally, Eqs. (3) are reduced to two second-order ordinary differential equations with the following solutions

$$\tilde{s}_{mm}^{(m,m)} = \frac{1}{L_1^{(m)}} f_1(c_m, s_m, \mathbf{l}_m)(\mathrm{W}_{11}^{(m)}\overline{s}_{11} + \mathrm{W}_{22}^{(m)}\overline{s}_{22}), \quad \tilde{s}_{12}^{(m,m)} = \frac{1}{L_2^{(m)}} f_2(c_m, s_m, \mathbf{l}_m)\mathrm{W}_{12}^{(m)}\overline{s}_{12}, \tag{4}$$

$$f_j(c_m, s_m, \mathbf{l}_m) = 1 - \cosh[\sqrt{L_j^{(m)}}(x_m - s_m)]\cosh^{-1}[\sqrt{L_j^{(m)}}(s_m - \mathbf{l}_m], \quad j = 1,2$$

Constants $L_1^{(m)}, L_1^{(m)}, \mathrm{W}_{11}^{(m)}, \mathrm{W}_{22}^{(m)}, \mathrm{W}_{12}^{(m)}$ depend on the stiffnesses $\hat{Q}_{ij}^{(m)}$ of the intact material of the m th layer, modified (due to the implicitly contained damage) stiffnesses $Q_{ij}^{(k)}, k \neq m$ of the equivalent constraint layer, shear lag parameters K_j and the layer thickness ratio c. In detail, they are presented in [22].

Stiffness Analysis

In order to determine the reduced stiffness properties of the damaged laminate, the reduced stiffness properties of the homogeneous layer, equivalent to the explicitly damaged ply, need to be determined first. Constitutive equations of the equivalent homogeneous layer have the form

$$\{\bar{s}^{(m,m)}\} = [Q^{(m)}]\{\bar{e}^{(m,m)}\} \tag{5}$$

The in-plane stiffness matrix $[Q^{(m)}]$ of the homogeneous layer, equivalent to the explicitly damaged m th ply, is related to the in-plane stiffness matrix $[\hat{Q}^{(m)}]$ of the pristine material via In-situ Damage Effective Functions (IDEFs) $\mathrm{L}_{22}^{(m)}$, $\mathrm{L}_{66}^{(m)}$ as

$$[Q^{(m)}] = [\hat{Q}^{(m)}] - [\hat{R}^{(m)}][\mathrm{L}^{(m)}] \tag{6}$$

$$[\hat{R}^{(m)}] = \begin{bmatrix} \hat{R}_{11}^{(m)} & \hat{Q}_{12}^{(m)} & 0 \\ \hat{Q}_{12}^{(m)} & \hat{R}_{22}^{(m)} & 0 \\ 0 & 0 & \hat{Q}_{66}^{(m)} \end{bmatrix}, \quad [\mathrm{L}^{(m)}] = \begin{bmatrix} \mathrm{L}_{22}^{(m)} & 0 & 0 \\ 0 & \mathrm{L}_{22}^{(m)} & 0 \\ 0 & 0 & \mathrm{L}_{66}^{(m)} \end{bmatrix}$$

$$\hat{R}_{mm}^{(m)} = \hat{Q}_{mm}^{(m)}, \quad \hat{R}_{22}^{(1)} = (\hat{Q}_{12}^{(1)})^2 (\hat{Q}_{11}^{(1)})^{-1}, \quad \hat{R}_{11}^{(2)} = (\hat{Q}_{12}^{(2)})^2 (\hat{Q}_{22}^{(2)})^{-1}$$

The lamina macrostresses $\{\bar{s}^{(m,m)}\}$ in the equivalent ply can be obtained by averaging the in-plane microstresses, Eq. (4), across the length of the representative segment as

$$\bar{s}_{mm}^{(m,m)} = \frac{1}{L_1^{(m)}}(1 - \tanh[\sqrt{L_1^{(m)}}(s_m - \mathbf{l}_m)])(\mathrm{W}_{11}^{(m)}\bar{s}_{11} + \mathrm{W}_{22}^{(m)}\bar{s}_{22}) \tag{7a}$$

$$\bar{s}_{12}^{(m,m)} = \frac{1}{L_2^{(m)}}(1 - \tanh[\sqrt{L_2^{(m)}}(s_m - \mathbf{l}_m)])\mathrm{W}_{12}^{(m)}\bar{s}_{12} \tag{7b}$$

The lamina macrostrains $\{\bar{e}^{(m,m)}\}$ are assumed to be equal to those in the equivalent constraint ply, i.e. $\{\bar{e}^{(m,m)}\} = \{\bar{e}^{(m,k)}\}$, as well as to the applied laminate strain, and are calculated from the constitutive equations for the equivalent constraint ply and the laminate equilibrium equations.

Substitution of Eq. (6) into constitutive equations, Eq. (5), for the equivalent homogeneous layer yields IDEFs in terms of the lamina macrostresses and lamina macrostrains as

$$\mathrm{L}_{22}^{(1)} = 1 - \frac{\bar{s}_{11}^{(1,1)}}{\hat{Q}_{11}^{(1)}\bar{e}_{11}^{(1,1)} + \hat{Q}_{12}^{(1)}\bar{e}_{21}^{(1,1)}}, \quad \mathrm{L}_{22}^{(2)} = 1 - \frac{\bar{s}_{22}^{(2,2)}}{\hat{Q}_{12}^{(2)}\bar{e}_{11}^{(2,2)} + \hat{Q}_{22}^{(2)}\bar{e}_{22}^{(2,2)}}, \quad \mathrm{L}_{66}^{(m)} = 1 - \frac{\bar{s}_{12}^{(m,m)}}{\hat{Q}_{66}^{(m)}\bar{g}_{12}^{(m,m)}} \tag{8}$$

Finally, closed-form expressions for IDEFs are obtained

$$\mathrm{L}_{qq}^{(m)} = 1 - \frac{1 - \mathrm{F}_q(D_m^{mc}, D_m^{ld})}{\dfrac{1 + b_q^{(m)} D_m^{ld}}{1 - D_m^{ld}} + g_q^{(m)} \mathrm{F}_q(D_m^{mc}, D_m^{ld})},$$

$$\mathrm{F}_q(D_m^{mc}, D_m^{ld}) = \frac{D_m^{mc}}{b_q^{(m)}(1 - D_m^{ld})} \tanh\left[\frac{b_q^{(m)}(1 - D_m^{ld})}{D_m^{mc}}\right], \quad q = 2,6 \tag{9}$$

Constants $b_q^{(m)}, g_q^{(m)}, q = 2,6, m = 1,2$ depend solely on the initial stiffnesses $\hat{Q}_{ij}^{(m)}$ of the m th layer, modified stiffnesses $Q_{ij}^{(k)}, k \neq m$ of the equivalent constraint k th layer, shear lag parameters K_j as well as the layer thickness ratio and are given in detail in [22]. The modified stiffnesses $Q_{ij}^{(k)}$ of the equivalently constraining k th layer are determined from the analysis of the ECMk laminate and are functions of the IDEFs $\mathrm{L}_{22}^{(k)}, \mathrm{L}_{66}^{(k)}$, depending explicitly on the damage parameters $D_k^{mc} = h_k / s_k$, $D_k^{ld} = \mathbf{l}_k / s_k$. Therefore, the IDEFs for both layers depend on each other. They form a system of four simultaneous nonlinear algebraic equations, which is solved computationally by a direct iterative procedure.

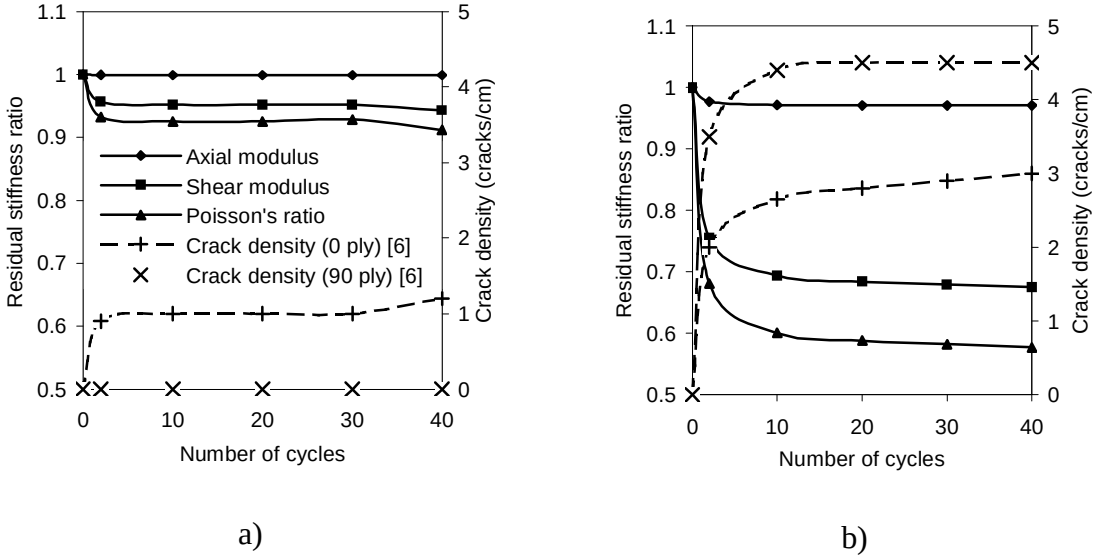

Figure 4. Stiffness reduction and damage development for a T300/914 $[0_4 / 90_4]_s$ laminate under thermal cycling: a) –200°C/ +20°C; b)–200°C/ +90°C

Results and Discussion

In absence of delaminations, the developed ECM/2-D shear lag approach has been validated by comparing its predictions with those obtained from the earlier developed models [17-19]. The results of comparison are published elsewhere [23].

Figure 4 shows observed damage development and predicted stiffness reduction in a cross-ply $[0_4/90_4]_s$ T300/914 carbon epoxy laminate during thermal cycling. Each cycle consisted of cooling at –200°C and heating at +20°C or +90°C, and crack density in the 90° and 0° plies was measured [15]. However the size of growing delaminations that accompanied longitudinal cracks in the –200° C/+90°C cycling was not. Predictions of reduction in the axial and shear moduli as well as the Poisson's ratio are shown along with the measured crack densities as a function of the number of cycles. During the $-200°C/+20°C$ cycling, (Fig. 5a), the predicted stiffness reduction is less than 10% for all stiffness properties due to zero crack density in the 90° ply. As transverse cracks developed during the $-200°C/+90°C$ cycling, the shear modulus and Poisson's ratio underwent up to 40% reduction. However, the predicted reduction of the axial stiffness in this case is less than 5%, Fig. 5b. This indicates that the shear modulus and the Poisson's ratio could be much better parameters to characterise stiffness degradation of the laminate than the axial modulus.

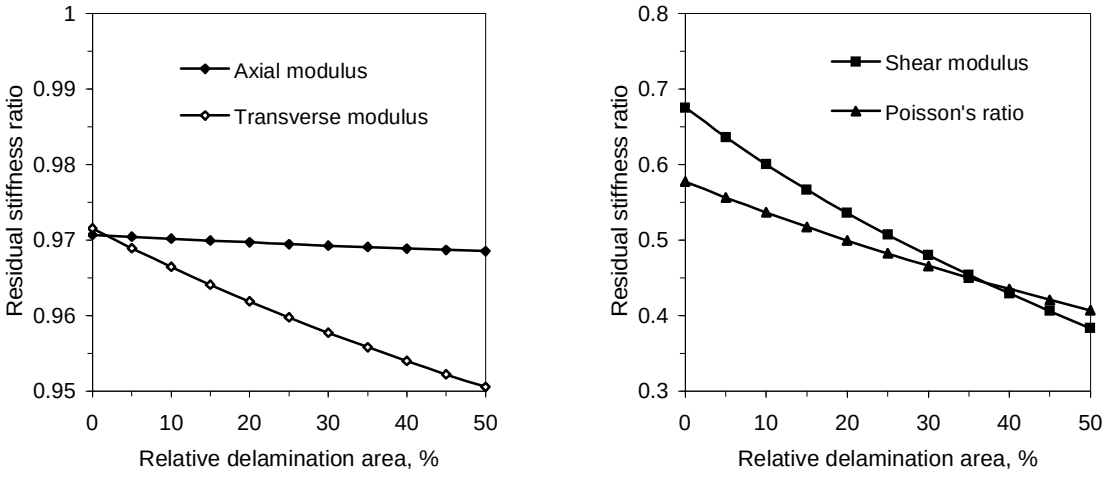

a) b)

Figure 5. Stiffness reduction of a T300/914 $[0_4/90_4]_s$ laminate as a function of the relative longitudinal delamination area after approximately 20 cycles at –200°C/ +90°C: a) axial and transverse moduli; b) shear modulus and Poisson's ratio. Crack densities (saturated values) in the 0° ply $C_1 = 3\,\text{crack/cm}$ and in the 90° ply $C_2 = 4.5\,\text{crack/cm}$.

Since the size of the delamination area was not measured during cycling, reduction of stiffness properties of $[0_4/90_4]_s$ T300/914 laminate due to delaminations was predicted using assumed delamination sizes. Strip-width of the transverse delamination was set to zero, while that of the longitudinal delamination allowed variation from zero to 50%. In other words, longitudinal delaminations were assumed to have propagated from the crack tip to one

quarter of the distance between two cracks. This seems to be a reasonable assumption, consistent with X-ray radiographs obtained in [7]. In Fig. 5, predicted reductions of the axial, transverse and shear moduli as well as Poisson's ratio are plotted as function of the relative delamination area. The axial modulus appear to be unaffected by the growth of delamination, while transverse modulus is further reduced, but not significantly, Fig. 4a. The reduction in the shear modulus is more pronounced than in the Poisson's ratio, Fig. 4b. Crack densities in 90^o and 0^o plies were taken as C_2=4.5 cracks/cm and C_1=3 cracks/cm respectively, which corresponds to saturation values reached during the $-200^oC/+90^oC$ cycling. Under uniaxial tensile loading, longitudinal delaminations appear to be more important than the transverse one, since they result in isolation of the portions of the load-bearing 0^o plies, which become prone to fibre breakage. Under biaxial tensile loading, the importance of one set of delaminations over the other depends very much on the biaxiality and ply thickness ratios. Recent work has extended the model to off-axis dominated laminates $[\pm\theta/0]_{ns}$ where matrix cracking and local delamination appear in the θ ply [16-17]. The challenge of course is to detect and measure the amount of damage that develops in the laminated structure non-destructively. This has been achieved in the laboratory environment on simple structural configurations [18-22] but further work is required.

STRUCTURAL HEALTH MONITORING (SHM) METHODS

The state of art of SHM methods amenable to the detection of the previous types of composite damage was reviewed. Two new evolving active structural health monitoring techniques, using piezoceramic actuators and sensors appear to show high sensitivity to small damage sizes. These are:

(1) active nonlinear acousto-ultrasonic based methods, and

(2) active Lamb wave based methods

Lamb wave methods are based on the principle of detecting changes in guided waves as they propagate through the material due to the presence of damage, and substantial efforts have been reported on these seemingly promising techniques [3, 9-10]. Yet, their application in detecting damage in composite materials and structures remains in many aspects an open field.

On the other hand, the nonlinear acousto-ultrasonic methods attempt to exploit the effect of anomalously high levels of nonlinearity in the material due to contact-type defects such as fracture cracks in the material. The nonlinear contact effects are typically accentuated by the superposition of a low frequency vibratory excitation with an ultrasonic signal. One widely used technique employs nonlinear modulation of ultrasonic waves by low-frequency vibration. In the frequency domain, the result of this modulation manifests itself as sideband spectral components with respect to the central frequency of the ultrasonic wave. This can be considered as a new signal generated by a defect, so the defect can be easily detected [11-19].

Distributed in-situ sensors and actuators. In the concept of the above stated SHM techniques, 3 types of in-situ sensors are identified and studied. Attached piezoceramic

wafers, or fibrous PZT films of the AFC (Active fiber composite) or MFC (macro fiber composite) type, fiber optic bragg gratings, and polymer resins hybridized with carbon nanotubes. The types of piezoceramic films provide good choices for the measurement of dynamic strains to frequencies up to several MHz. FBGs have been also developed capable of measuring dynamic strain up to the MHz range. They can be easily embedded into the composite. Finally, hybridized matrices with CNT nanoparticles have shown sensitivity to strain and damage and can provide an alternative way for detecting damage in composite materials. In terms of actuators, it seems that piezoceramic actuators in the form of solid state wafers or AFC/MFC films provide the best choice for inducing dynamic strains in frequencies up to the MHz range. Due to the availability of hardware, preliminary conducted work, described in the next task, was focused on piezoceramic actuators and sensors.

Based on the conclusions of the above study, ***a novel active nonlinear acousto-ultrasonic piezoelectric sensor (ANAUPS)*** was proposed and devised in Task 2, and preliminary experimental work was conducted to investigate its feasibility and potential. This novel ANAUPS and the associated SHM method, will apparently combine benefits of the nonlinear acousto-ultrasonic SHM techniques and piezoelectric wafer/film transducers.

TASK 2: Damage Detection and Characterization

The scope of this task was the preliminary exploration of the potential of new non-linear acousto-ultrasonic SHM methodologies for detecting damage in composite materials. The implementation of multiple piezoelectric actuators and sensors to generate and acquire the propagation of low and high frequency waves was an apparent objective. As mentioned above development of methodologies capable to detect and localize damage receive current attention. In recent years a range of different techniques based on propagation of elastic waves were presented and are summarized by Staszewski [29]. These techniques have the benefit of damage detection in large structures using a small number of transducers. Soutis and coworkers have presented lamb wave based methods for the detection of damage in composite structures [1-2]. An analytical and experimental approach for damage detection in composite structures was presented by Giurgiutiu [30] using piezoelectric wafers to generate Lamb waves in metallic structures. Additionally, a new methodology for detecting damage in thin walled plate metallic structures, using 2-D ultrasonic phased arrays, was presented, obtaining beam-forming signals in various directions within the 360^{o} full range [31]. A Lamb wave methodology for detection of delamination and matrix cracking in composite structures using piezoelectric actuators and sensors was presented [3]. Chrysochoidis and Saravanos [32] presented analytical and experimental work on the high frequency wave propagation in delaminated composite beams examining the effect of various delamination crack length on wave propagation and the time-frequency field.

Exploitation of nonlinear vibro-acoustic effects for diagnostics and, in particular, for early crack detection is an emerging technique, which is rapidly progressing during last several years after pioneering encouraging results [33-34]. These Nonlinear elastic wave spectroscopy methods are summarized from Van den Abeele et al.[35-36] and appear to be

powerful new tools in interrogation of damage in materials. Due to material nonlinearity, a wave can distort, creating accompanying harmonics, multiplication of waves of different frequencies, and, under resonance conditions, changes in resonance frequencies as a function of drive amplitude. In undamaged materials, these phenomena are very weak. In damaged materials, they are remarkably large. The sensitivity of nonlinear methods to the detection of damage features (cracks, flaws, etc.) is far greater than that of linear acoustical methods (measures of wave speed and wave dissipation), and in fact, these methods appear to be more sensitive than *any* method currently available [37-39]. One non linear wave spectroscopy method depends on the study of a single mode within the material. In this case resonance frequency shifts, harmonics, and damping characteristics are analyzed as function of the resonance peak acceleration amplitude consisting indices of the structural health condition [40]. A widely used methodology is based on monitoring nonlinear wave mixing in the material. Two excitation signals are used, examining the modulation of the weaker wave under the action of a strong low-frequency wave or vibration. The manifestations of the non linear response appear as wave distortion and generation of additional harmonics (sidebands). Various experimental setups have been used to generate non-linearities under the low frequency excitation like impact hammers, mechanical actuators [43], speakers and piezoceramic materials [44]. Additionally non linear wave modulation techniques are widely used to detect crack in metallic structures [43], machine components,[41], adhesive joints [42] polymers [35] and more recently matrix cracks in composite materials. However, very little work has been done in the area of detecting delamination in composite structures using non linear wave spectroscopy methodologies [45].

To this end, in order to examine the feasibility of delamination detection via non-linear ultrasonics, preliminary experiments were conducted at the University Patras (UoP) and results were obtained. These experiments were focused on the detection of small delamination cracks artificially induced during the fabrication of Glass/Epoxy strips and demonstrated the feasibility of detection of interlaminar cracks in composite beams through a nonlinear acousto-ultrasonic method. Additionally a “pitch and catch” configuration is used to generate and acquire Lamb waves across delaminated beams studying their sensitivity to reveal damage presence.

MATERIALS AND EXPERIMENTAL SETUP

Experiments were contacted on Glass-fiber/epoxy (GFRP) laminated plates using 16 layers of glass-fiber woven fabric (200 g/m^2) in epoxy resin in order to produce 4.48 mm total thick beams with $[0/90/90/0]_{16}$ laminations, 396 mm long and 30 mm wide. Three different specimens were tested; one baseline pristine specimen; a specimen with artificially created full width 40mm long delamination crack using a PTFE-film during the fabrication procedure; and a beam with a created delamination crack with length approximately 30mm. The experimental setup is illustrated in Fig. 6. The specimens were tested under free-free supporting conditions. An *Active Nonlinear Acousto-Ultrasonics Piezoelectric Sensor (ANAUPS)* was devised consisting of three piezoceramic (PZT5) patches, polarized in the

thickness direction, which were attached on the beam's surface, one acting as a sensor and the other two as actuators. The first actuator was excited with a low frequency sine wave to generate nonlinear interactions between the delamination faces. Additionally, a second actuator-sensor pair was used to generate and monitor a high frequency signal in the ultrasonic regime. In the case of

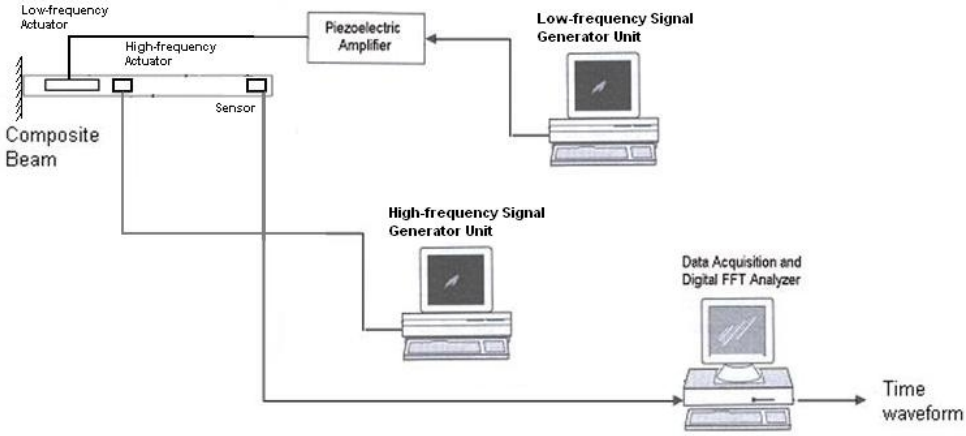

(a)

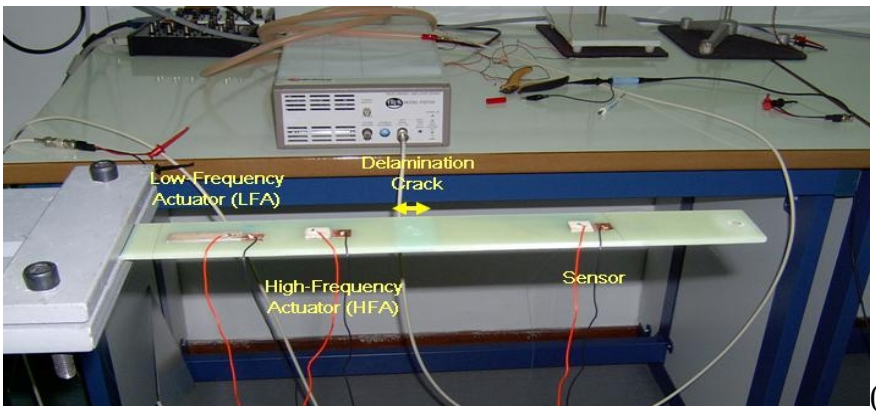

(b)

Figure 6. Experimental Setup

Lamb wave generation, a narrow-band Gaussian pulse was used. The sensory voltage was acquired via an ultra high frequency data acquisition board. Frequency content was extracted using a Fast Fourier Transformation (FFT); alternatively, time-frequency pseudo Wigner-Ville distributions (PWVDs) were extracted from the time signal, as required.

RESULTS AND CONCLUDING REMARKS

Active Nonlinear Acousto-Ultrasonics Piezoelectric Sensor (ANAUPS)

Preliminary tests were conducted for various high frequency excitations in order to investigate the ability of the ANAUPS and the related nonlinear acoustics methodology to

detect delamination crack presence in composite active sensory beams. Three different frequency levels were selected for the sine signal, which provided the high frequency excitation; 20, 30 and 80 KHz. Additionally non linear phenomena from the damage region were excited via a low frequency sine signal applied at the second piezoceramic actuator. The 1st resonance frequency was selected for the low frequency case, while amplitude of the applied signal was 480Volt. In order to assess the effect of delamination on the acoustical spectral components, experiments were performed on a healthy baseline specimen, the specimen with 30 and 40 mm delamination length cracks, as described previously.

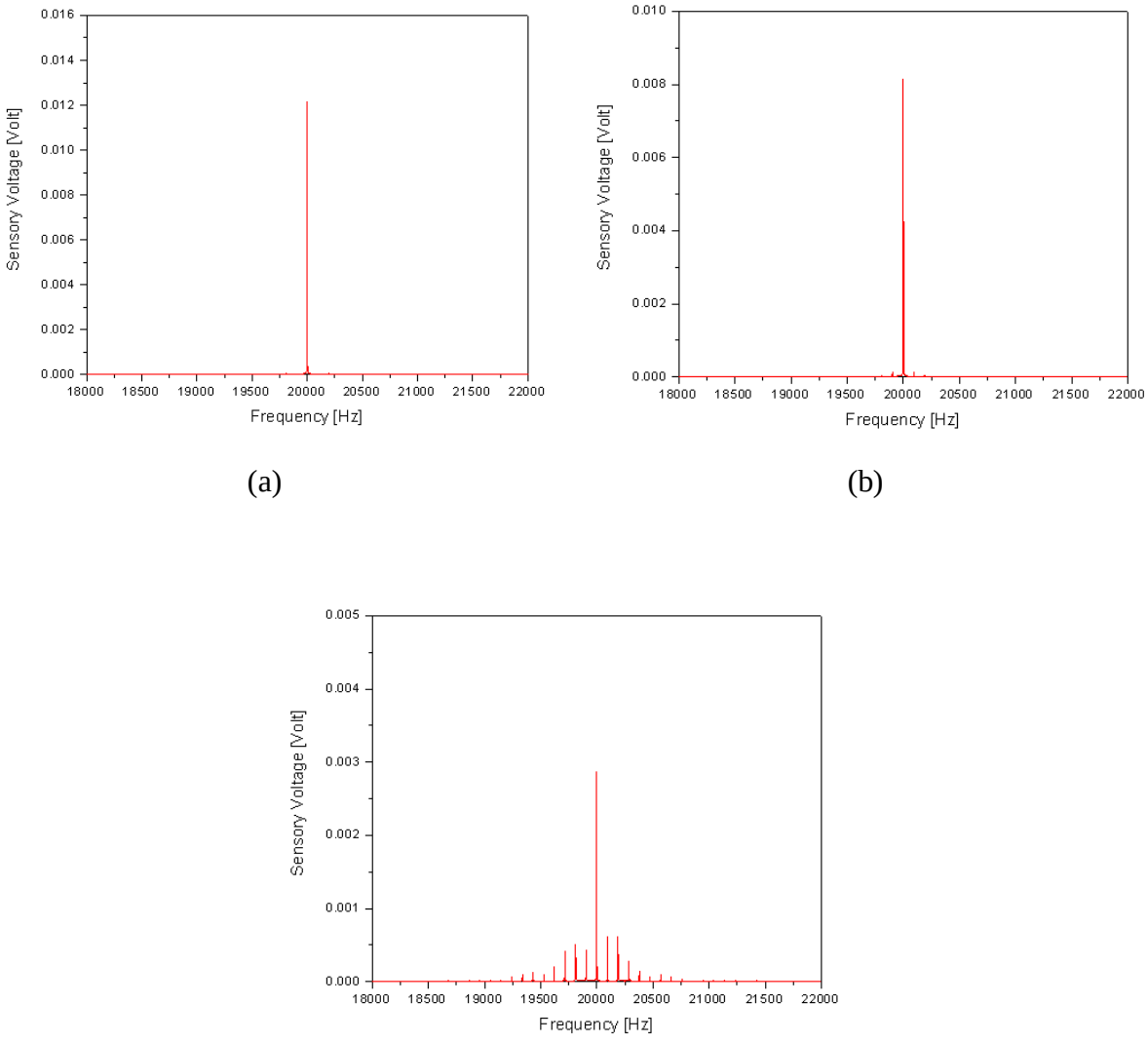

Figure 7. Power spectra of ultrasonic responses at 20 kHz and 480 Volts amplitude for (a) the healthy specimen and, (b) specimen with approximately 30mm delamination and (c) beam with 40mm delamination debonding.

Delamination Detection Potential. The results for each high frequency excitation are presented in Figs. 7-9, for the 20, 30 and 80 KHz applied signals respectively. The ultrasonic carrier frequencies of 20, 30, and 80 KHz can be observed in all presented spectra. A clear pattern of sidebands around the carrier frequency is observed in the measurements for the specimen with the large delamination size, while for the smaller delamination crack size only

for the 80 KHz excitation frequency there is sensitivity to the delamination existence. This conclusion indicates that probably a relation exists between delamination size and the excitation frequency to reveal the damage. This conclusion can be used for extracting information about the damage size in the structure.

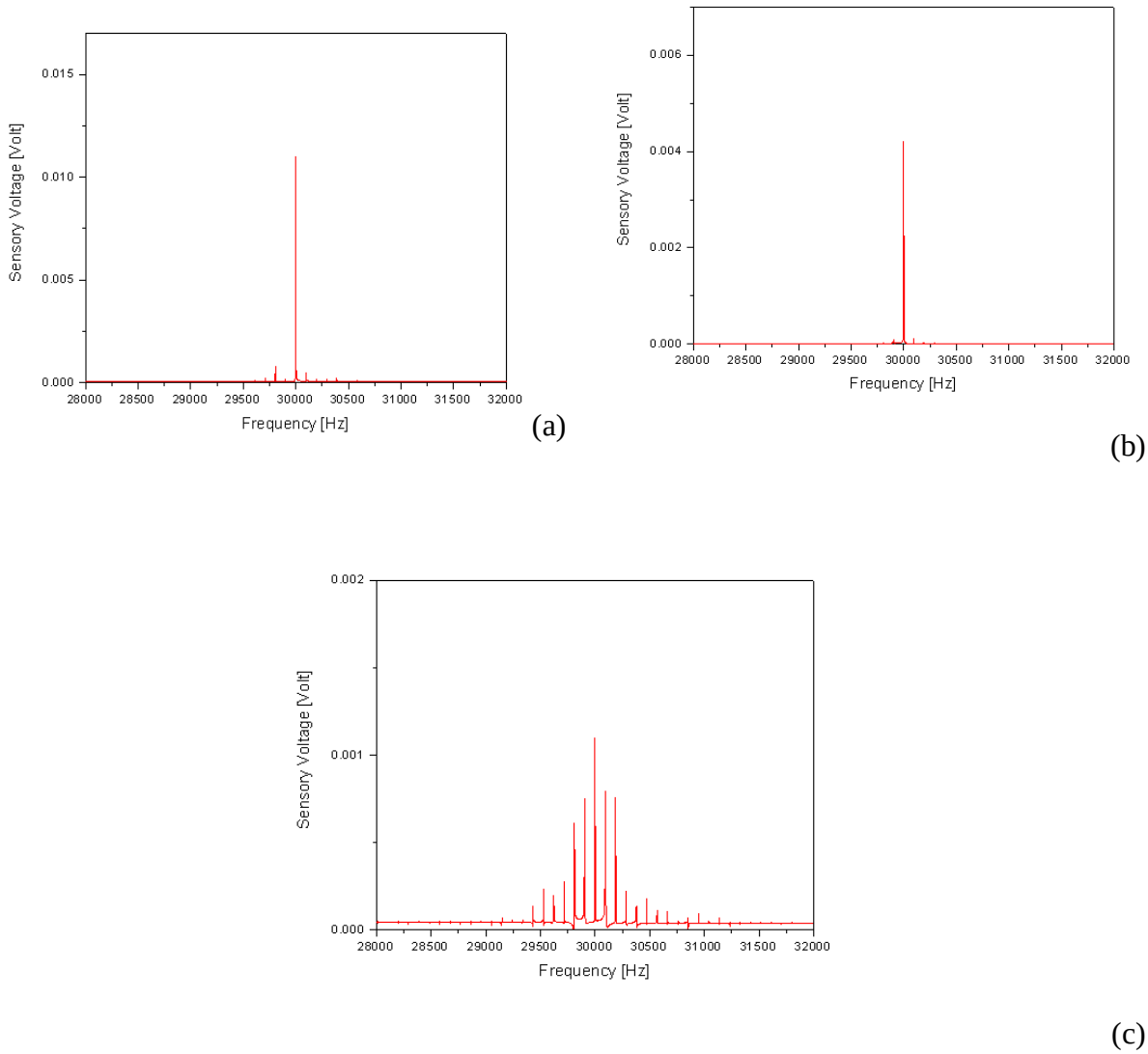

Figure 8. Power spectra of ultrasonic responses at 30 kHz and 480 Volts amplitude for (a) the healthy specimen and, (b) specimen with approximately 30mm delamination and (c) beam with 40mm delamination debonding.

However, the absence of nonlinear spectral components in the healthy baseline specimen enforces the capability of the proposed methodology to monitor delamination cracks without requiring of pristine specimen as a reference state. Additionally the amplitude of the central carrier peak can be used as a second damage indicator, which was found to be related mostly on linear wave attenuation. For both delamination cases, the amplitude of the central peak is reduced compared with the measurement of the healthy beam.

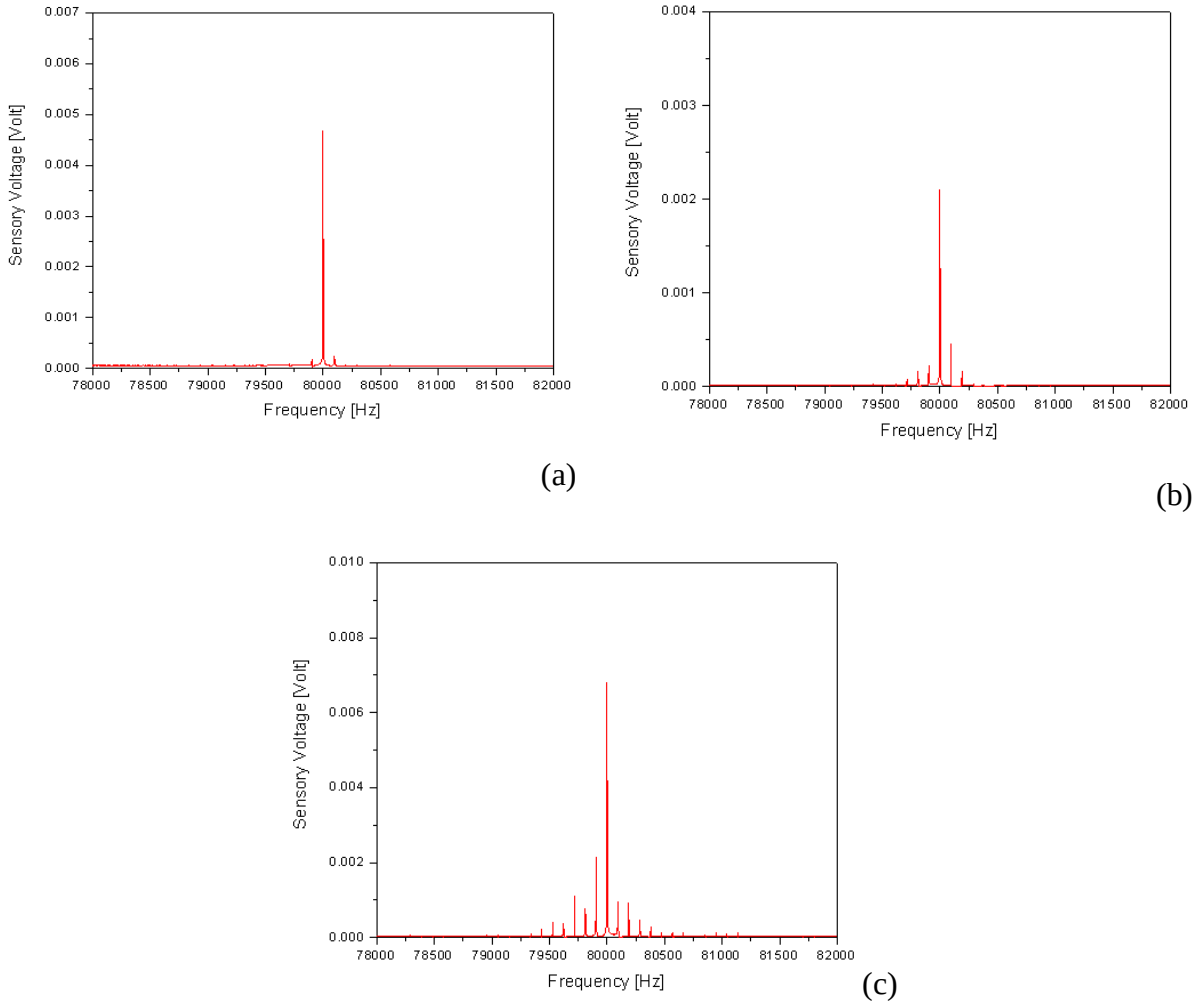

Figure 9. Power spectra of ultrasonic responses at 80 kHz and 480 Volts amplitude for (a) the healthy specimen and, (b) specimen with approximately 30mm delamination and (c) beam with 40mm delamination debonding.

The damage index seems to be highly sensitive to small delamination size, but it requires additional information for a baseline healthy beam.

Effect of Low-Frequency Signal Amplitude. In this section, the effect of the amplitude of the low-frequency signal applied on the actuator on the measured sensory response is being examined. The results in Fig. 10 present the sensitivity of the sideband spectrum components as a function of the low frequency excitation amplitude. Three different gains were tested, 0,240 and 480 Volt. As the voltage amplitude of the excitation increases, the amplitude of the central peak corresponding to the ultrasonic carrier frequency reduces.

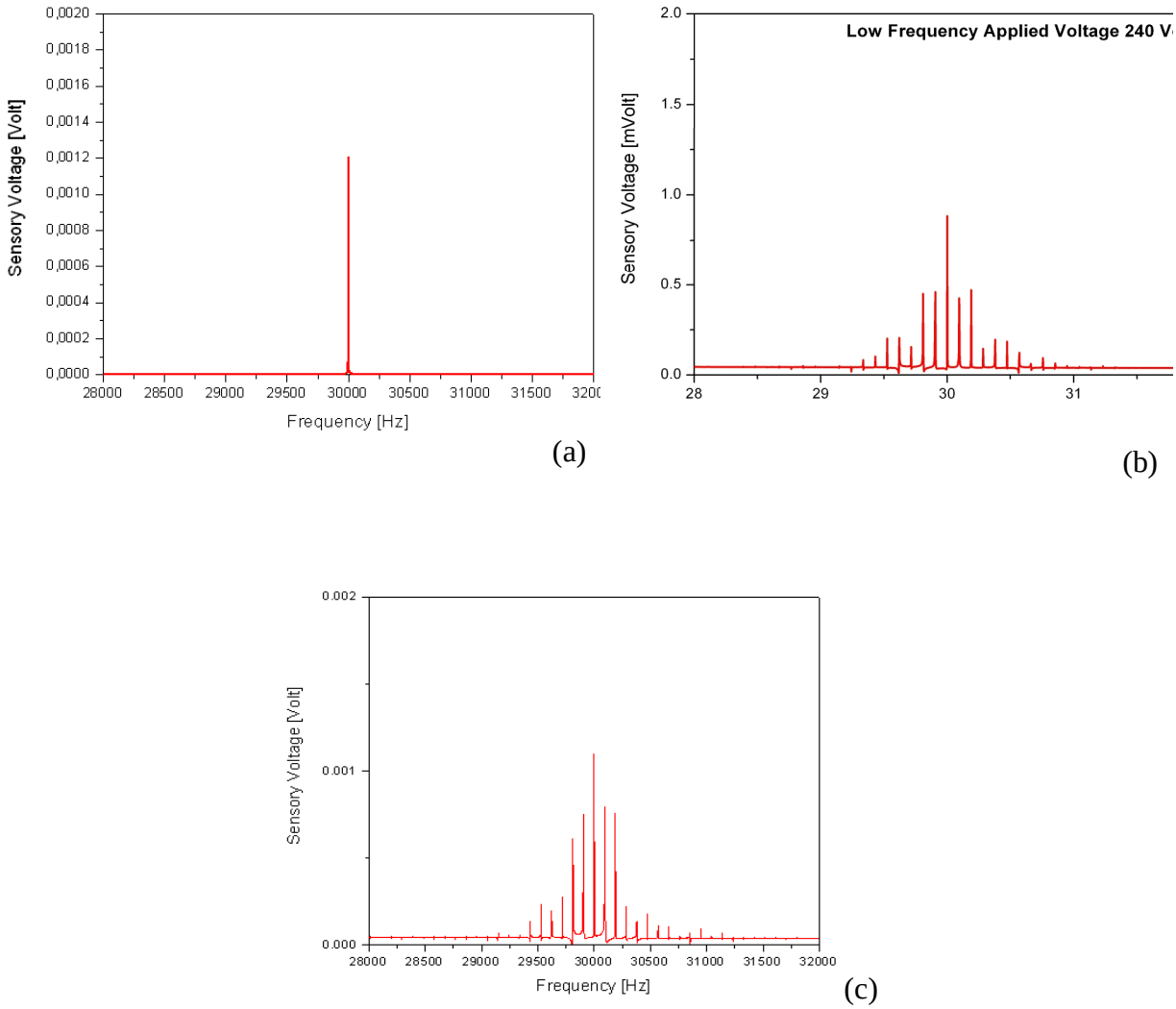

Figure 10. Power spectra of ultrasonic responses for a specimen with 40mm delamination crack for applied low frequency voltage (a) 0 Volt , (b) 240 Volt and (c) 480Volt.

The energy of the carrier component seems to transfer to the sidebands, resulting in a larger number of sidebands with higher amplitudes. This shows that the spectral intensity increases as the voltage amplitude of the piezoelectric low frequency excitation.

IDENTIFIED KEY OPEN ISSUES

The preliminary work in Task 2 has provided valuable insight regarding the feasibility and potential of ANAUPS, however, it has also identified key open issues in this area, which should be further explored:

- How the observed sideband spectrum relates to size, location and type of damage?

- How the selection of LFA and HFA excitation in terms of waveform type, frequency and energy content, (also the placement and size of the actuators and sensors) affects the sideband spectrum?
- Can the method detect matrix cracks?
- What is the sensitivity of the method, range of detection?

TASK 3: Composite Material Modeling for SHM and Simulation for Life Prediction

One of the objectives of this task was to explore the development of new modeling tools enabling simulation of the response of a composite structure SHM system, with embedded actuators and sensors inclusive of the presence of damage. The envisioned models will build on previous background of the collaborating teams and will include:

- Formulation of new internally scalable and adaptable generalized laminate theories inclusive of piezoelectric layers, interlaminar cracks and contact effects, which will provide the core of the method. The new laminate models will involve high-order layerwise approximations in the thickness direction for all displacements and electric state variables, will explicitly satisfy state and shear stress continuity at pristine ply interfaces and will encompass natural contact and sliding conditions at debonded ones. The laminate models will be capable to duplicate the accuracy of exact wave propagation solutions in the thickness direction. In addition, they will entail the capability to model nonlinear contact effects at delaminations and analyze the behavior of the proposed nonlinear acousto-ultrasonic SHM configurations. Finally, the proposed models will yield the fidelity of stress prediction at interfaces required by the life prediction models in Objective 3.
- Development of semi-analytical methods for the prediction of the wave propagation in composite strips and plates, which will encompass the previously described laminate models in the thickness direction, yet, entailing exact solutions in the planar directions.

In this context, a previously developed layer-wise FE for delaminated composite beams with piezoelectric actuators and sensors was further expanded to include contact effects at the delamination interfaces such that it can provide a first modeling platform for predicting and quantifying the non-linear ultrasonic response observed in the experimental measurements of Task 2.

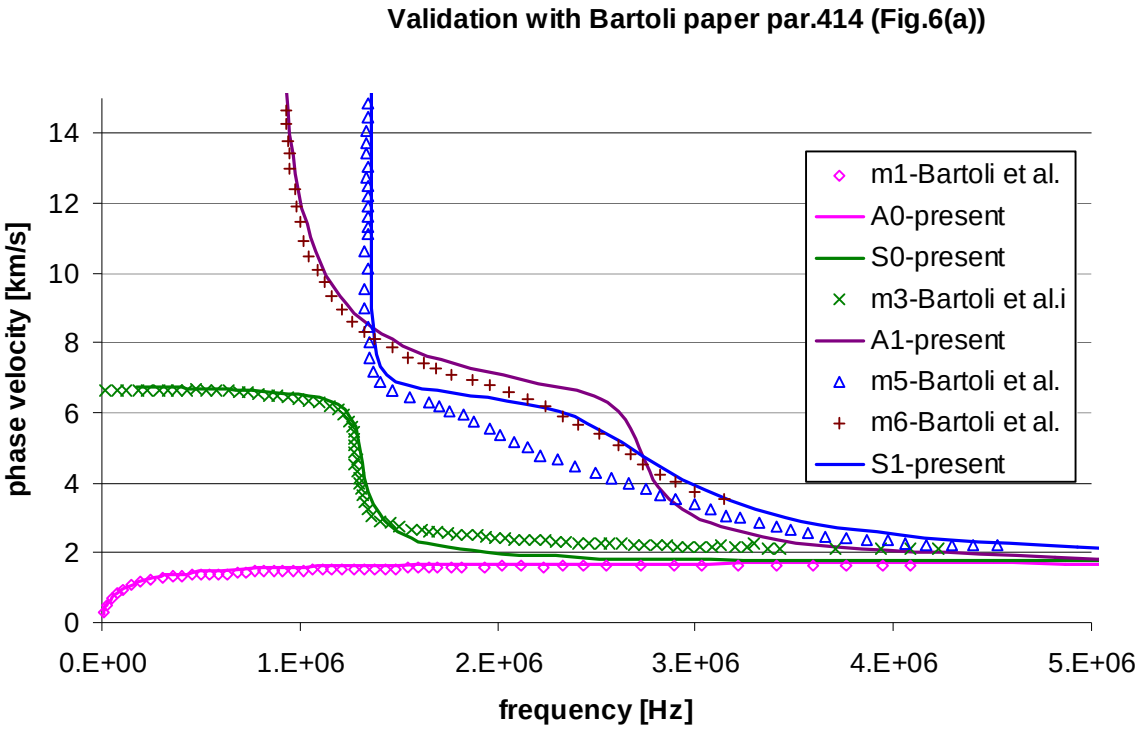

Figure 11. Dispersion curves obtained through a layerwise semi-analytical solution for a Carbon/Epoxy beam with $[45/-45/0/90]_s$ lay-up (solid lines) and comparison with results reported by Bartoli et al. [46].

Also, a semi-analytical wave propagation solution for laminated composite strips was formulated, implementing a linear layerwise laminate theory [47] in the thickness direction together with an exact wave propagation solution in the planar direction. Numerical results were obtained for the case of laminated strips which demonstrate the feasibility of the concept and the versatility of the layerwise models in yielding wave propagation solutions in composite beams of various laminations. Figure 11 shows typical predicted dispersion curves in a Carbon/Epoxy composite strips with $[45/-45/0/90]_s$ lay-up using 31 discrete layers. The numerical results were found to be in very good agreement with those reported by Bartoli et al. [46], and easily predicted the through-thickness anti-symmetric and symmetric wave modes.

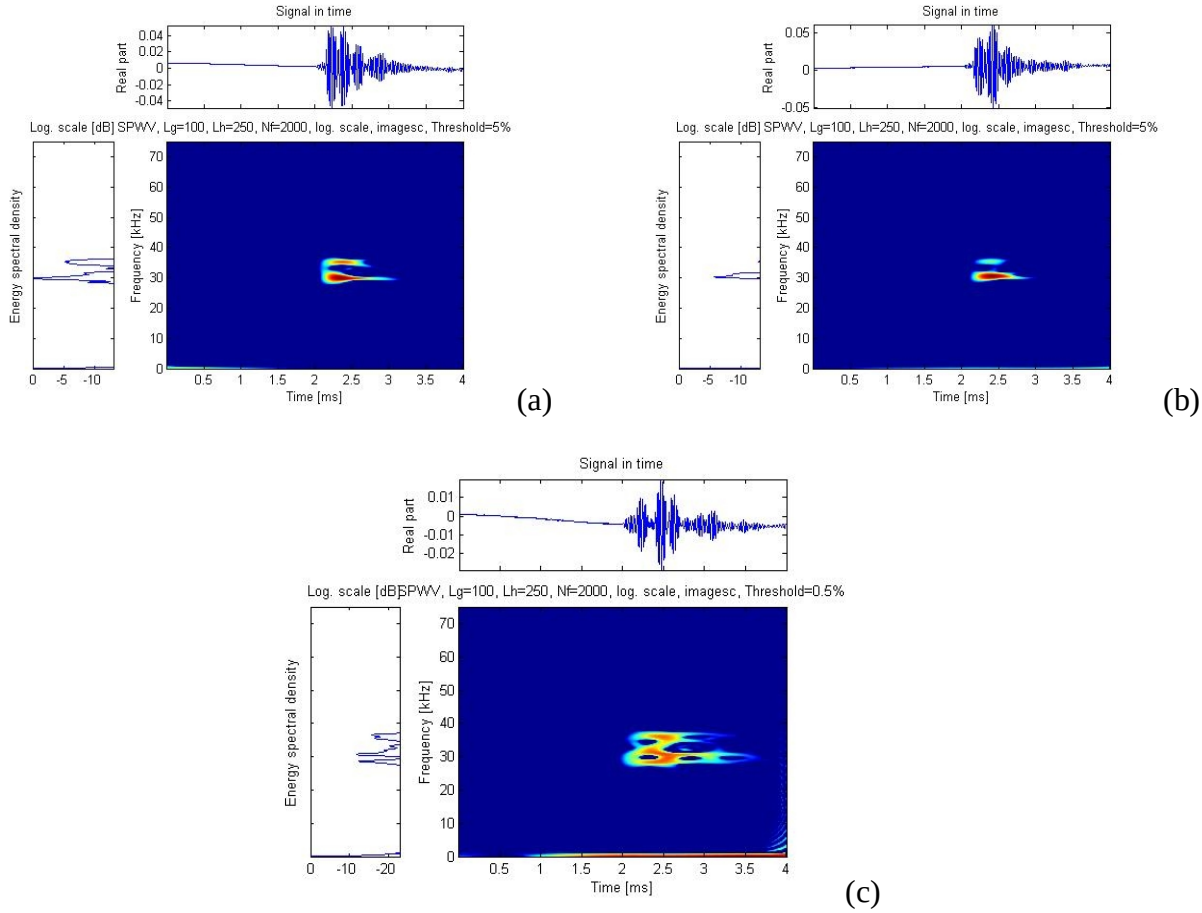

Figure 12. Time-Frequency distribution of a propagated A_0 antisymmetric Lamb mode across composite specimens (a) without delamination crack (b) with a delamination crack covering approximately 30mm and (c) with a 40mm delamination crack.

LAMB WAVE BASED DETECTION

To this end, using the semi analytical solution described above, the propagation of symmetric and antisymmetric modes across delaminated beams was additionally studied. In this case a different experimental setup was used, where the high-frequency piezoceramic actuator-sensor pair was used to generate and monitor Lamb waves in a pitch and catch configuration. The second actuator (used as low frequency actuator earlied) was not used in this study. The objective of this study is to investigate the Lamb wave propagation in the damaged and baseline specimens and compare with the nonlinear ultrasonic method. The healthy baseline and delaminated specimens were excited with a Gaussian pulse at two different frequencies of 32 kHz and 140 kHz, selected respectively for the generation of A_0 and S_0 type Lamb waves. Time-frequency distributions were extracted using pseudo Wigner-Ville Transformation in order to examine how the frequency content of the signal changes as a function of time. Figs. 12-13 illustrate time and time-frequency distributions for the selected narrowband excitation at 32 kHz (A_0 mode) and at 150 kHz (S_0 mode) for both the pristine and the delaminated composite beams.

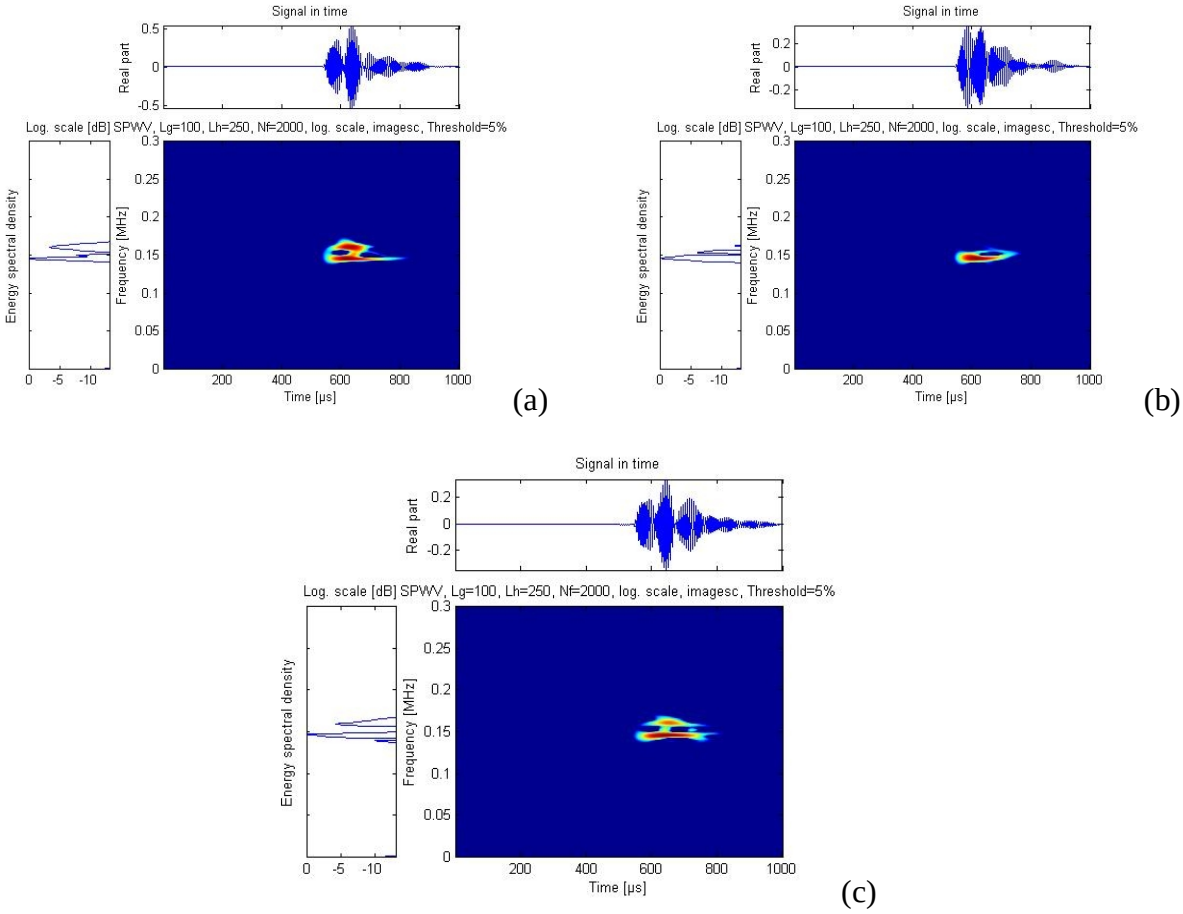

Figure 13. Time-Frequency distribution of a propagated S_0 antisymmetric Lamb mode across composite specimens (a) without delamination crack (b) with a delamination crack covering approximately 30mm and (c) with a 40mm delamination crack.

The existence of delamination probably seems to affect the propagation of the antisymmetric (A_0) mode at 32 kHz and the symmetric (S_0) mode at the 150 kHz. In both excitation cases the delamination crack has no significant effect on the time of flight. However, in both excitations, the time signal of the delaminated beam is being separated into two different wave packets. In both cases, the delamination reduces the amplitude of the first packet. The amplitude range and time delay of the second packet strongly depend on the excitation frequency. It is observed that in the high frequency excitation (150 kHz) the second wave packet becomes more dominant. The reasons for this effect will be analyzed and explained in future work. PWVD time-frequency responses obtained by the measured time signals are also sensitive to the damage presence. The central spectral frequency of the delaminated specimen is increased with respect to the baseline specimen, for the low frequency case. On the contrary, for the high frequency case the central spectral frequency of the damaged specimen is reduced. While the sensor signal seems to detect the presence of this small size delamination, one may say that a baseline reference is required in order to extract safe results. Further investigations seem to be required to clarify the effect of Lamb wave propagation in delaminated composite structures.

It can be seen that the preliminary results demonstrate that the development of novel layerwise laminated models can provide a powerful theoretical framework which may yield:

- either semi-analytical wave propagation models, through proper formulations, which will provide valuable numerical results for designing the SHM system, in terms of excitation frequency ranges, phase and group velocities, propagation of select symmetric and anti-symmetric wave modes, and optimal sizes for actuators and sensors capable to excite guided wave propagation in the composite structure, or
- specialty finite elements which will provide sufficient through-thickness detail and fidelity required for the modeling of damage propagation and residual stiffness, residual strength estimations of the composite structure. Transverse matrix cracking and longitudinal splitting can reduce the axial stiffness of the laminate but more importantly the shear modulus where reductions of up to 40% have been observed, Fig.4 [14].

IDENTIFIED KEY OPEN ISSUES

The preliminary work in this Task has provided valuable insight regarding the modeling of the envisioned SHM system and the life prediction of composites, however, it has also identified key open issues in this area, which should be further explored:

- Can we expand the semi-analytical wave propagation solution to encompass actuators, sensors and damage?
- Can we model and quantify the behavior nonlinear acousto-ultrasonic SHM system?
- Can we design an effective and sensitive SHM systems for a given type/size of damage? Predict the POD?
- Can we quickly predict the degradation in residual stiffness and strength for a given detected damage?

TASK 4: Specification of new Damage Tolerant Strategies

The specification of new damage tolerant strategies for composite structures is not a straight forward task. However, one can claim that the work and exploratory results conducted and obtained in the previous tasks, alone, suggests the key objectives which if properly addressed in future work, may lead to new strategies and design paradigms for damage tolerant composite structures. These **key objectives** and their envisioned synergistic combination are shown in Figure 14. **The 5 research objectives clearly provide the motivation for future**

work, and will be addressed in a future full-length proposal which will be the continuation of this exploratory grant, as described in Task 5.

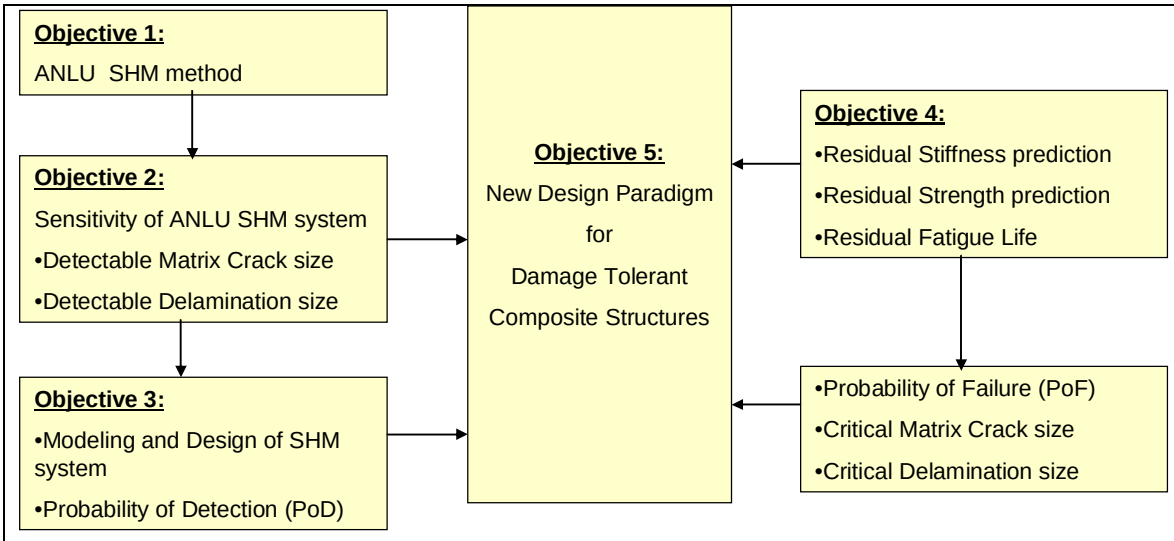

Figure 14. A possible design strategy leading to new damage tolerant composite structures, and related research objectives.

Task 5: Synthesis of Results and Proposed Future Work

A white paper was delivered to Dr. Victor Giurgiutiu (AFOSR), outlining a plan of future work in this topic. The white paper was approved and a stage 2 full length proposal will be submitted and is currently under preparation.

A Full length proposal is currently under preparation to be submitted by 30th of April 2009.

2. RESULTANT INTERACTIONS, PRESENTATIONS AND PUBLICATIONS

According to the planed project meetings:

- Prof. Saravanos visited University of Sheffield on 18th of December 2008. The aim of this trip was to review current progress, outline future work and synergistic collaborations between the two partners, and prepared the first proposal outline.
- Prof. Soutis visited UoP on 16th of February 2009, for the second project meeting,
- Both Profs Soutis and Saravanos visited WPAFB in Dayton Ohio on the 2nd of March 2009 and presented the final project findings. The presentation was well attended by several WPAFB research scientists and engineers, including AFOSR Structural Mechanics Program Managers: Dr V. Giurgiutiu and Dr. D. Stargel. After the presentation they had technical discussions with key personnel from the Materials Manufacturing Directorate and more specifically the non metallic materials division and the metals, ceramics and the NDE divisions.

Publications:

A conference paper containing results obtained during this exploratory EOARD grant was presented at the SPIE Smart Structures/NDE conference, San Diego California, 8-12 March 2009 with title "On the Delamination Detection in Composite Beams with Active Piezoelectric Sensors using non-linear Ultrasonics" by Nikos A. Chrysochoidis and Dimitris A. Saravanos [48]. Both teams (UoS, UoP) will present at the 10th International Conference of Deformation & Fracture of Composites, 15-17 April 2007, Sheffield, UK http://www.shef.ac.uk/materials/conferences/dfc10/index.html

3. REFERENCES

1. Diamanti, K., Soutis, C. and Hodgkinson, J. M., Composites A, **38**(4), (2007), 1121-1130.
2. Diamanti, K., Soutis, C. and Hodgkinson, J. M., Composites Science & Technology, **65**(13), (2005), 2059-2067.
3. S.S. Kessler, S. M. Spearing and C. Soutis, Smart Materials and Structures **11**(2), (2002), 269-278.
4. S. S. Kessler, S. M. Spearing, M. J. Atalla, C. E. S. Cesnik and C. Soutis, Composites Pt. B, **33**, (2002), 87-95.
5. Kashtalyan, M and Soutis, C., Composites A, **38**(4), (2007), 1262-1269.
6. Kashtalyan M. and Soutis, C., Progress in Aerospace Sciences, **41**(2), (2005), 152-173.
7. Soutis, C and Guz, I.A., The Aeronautical Journal, **110**(1105), (2006), 185-195.
8. Edgren, F., Soutis, C. and Asp, L.E., To appear in Composites Science & Technology, (2008).
9. Parvizi, A., Garret, K.W., and Bailey, J.E., *J. Mat. Sci.*, Vol. 13, 1978, pp. 195-201
10. Daniel, I.M., and Charewicz, A., *Eng. Fracture Mechanics*, Vol. 25, Nos. 5-6, 1986, pp. 793-808
11. Jamison, R.D., Schulte, K., Reifsnider, K.L., and Stinchcomb, W.W., Characterization and Analysis of Damage Mechanisms in Tension-Tension Fatigue of Graphite/Epoxy Laminates, *Effects of Defects in Composite Materials, ASTM STP 836*, American Society for Testing and Materials, Philadelphia, 1984, pp. 21-55
12. Smith, P.A., Wood, J.R., *Composites Science and Technology*, Vol. 38, No. 1, 1990, pp. 85-93
13. Charewicz, A., and Daniel, I.M., Damage Mechanisms and Accumulation in Graphite/Epoxy Laminates, *Composite Materials: Fatigue and Fracture, ASTM STP 907*. H.T. Hahn, Ed., American Society for Testing and Materials, Philadelphia, 1986, pp. 274-297
14. Boniface, L., and Ogin, S.L., *J. Comp. Materials*, Vol. 23, 1989, pp. 735-754
15. Henaff-Gardin, C., Lafarie-Frenot, M.C., and Gamby, D., *Comp. Structures*, Vol. 36, 1996, pp. 131-140
16. Ogin, S.L., Smith, P.A. and Beaumont, P.W.R., *Comp. Sci. Tech.*, Vol. 22, 1985, pp. 23-31
17. Hashin, Z., *Trans. ASME J. Applied Mechanics*, Vol. 54, 1987, pp. 872-879
18. Tsai, C.L., and Daniel, I.M., *Int. J. Solids and Structures*, Vol. 29, 1992, pp. 3251-3267
19. Henaff-Gardin, C., Lafarie-Frenot, M.C., and Gamby, D., *Comp. Structures*, Vol. 36, 1996, pp.113-130
20. Kashtalyan, M., and Soutis, C., *Adv. Comp. Letters*, Vol. 8, 1999, pp. 149-156
21. Zhang, J., Fan, J., and Soutis, C., *Composites*, Vol. 23, 1992, pp. 291-298
22. Kashtalyan, M., and Soutis, C., *Composites Part A*, Vol. 31, 2000, pp. 107-118
23. Kashtalyan, M, and Soutis, C., *Composites Part A*, Vol. 31, 2000, pp. 335-351
24. Kashtalyan, M and Soutis, C. *Journal of Materials Science*, 41(20), 2006, pp.6789-6800.
25. Diamanti, K., Hodgkinson, J.M. and Soutis, C. *Structural Health Monitoring* journal, 3(1), (2004), 33-41.
26. Qiu, Z-X., Yao, X-T., Yuan, J. and Soutis, C. *Smart Materials & Structures*, 15(4), (2006), 1047-1053.
27. Soutis, C. and Diamanti, K. *The Aeronautical Journal*, 112(1131), (2008), 279-283.
28. Saravanos, D. A. and Hopkins, D. A., J. of Sound and Vibration 192(5) (1996), 977-993.
29. Staszewski, W. J., "Structural health monitoring using guided ultrasonic waves", Advances in Smart Technologies in Structural Engineering, Holnicki-Szulc, J. and Mota-Soares, C. A., Berlin, Springer, 117-162 (2004).
30. Giurgiutiu, V., J. Intelligent Material Systems and Structures 16(4), (2005),291-305.
31. Lingyu, Yu and Giurgiutiu, V., Ultrasonics 48(2), (2008) 117-134.

32. Chrysochoidis, N. and Saravanos, D. A., Journal of Intelligent Material Systems and Structures, In press.
33. Buck O, Morris WL and Richardson JM. Applied Physics Letters;33(5), (1978),371–378
34. Antonets VA, Donskoy DM, Sutin AM. ,Mech Compos Mater ;(5), (1986),934–937.
35. Van Den Abeele, K.E. , Johnson P.A. and Sutin, A., Research in Non Destructive Evaluation, 12(1), (2000) 17-30
36. Van Den Abeele, K.E. , Carmeliet,J. Ten Cate J.A. And Johnson P.A., Research in Non Destructive Evaluation, 12(1), (2000), 31-42
37. Nagy, P.B., Ultrasonics 36, (1998), 375-381
38. J. H. Cantrell and W. T. Yost. *Phil. Mag.* A69:315 (1994).
39. Zaitsev, V., Nazarov V., Gusev, V. and Castagnede, B., NDT & E International 39, (2006), 184-194
40. Cantrell J.H. and Yost W.T., Internation Journal of Fatigue 23, (2001),S487-S490
41. Zagrai, A., Donskoy, D., Chudnovsky, A. and Golovin, E., Research in Nondestructive Evaluation,19(2), (2008) 104 -128
42. Hirsekorn,S., Ultrasonics, 39, (2001),57-68
43. Donskoy, D., Sutin, A. and Ekimov, A., NDT & E International 34(4), (2001), 231-238.
44. Parsons, J. and Staszewski, W. J., Smart Materials and Structures 15(4), (2006) 1110-1118.
45. Solodov,I. and Busse, G., Applied Physics Letters 91,251910 (2007)
46. Bartoli I., Marzani A., Lanza di Scalea F. and Viola E., J. of Sound and Vibration **295** (2006) 685–707.
47. Saravanos, D.A., Heyliger, P.R. ,Journal of Intelligent Material Systems and Structures **6** (3),(1995), 350–363.
48. Chrysochoidis, NA, Barouni, AK. and Saravanos, D.A., On the delamination detection in composite beams with active piezoelectric sensors using non-linear ultrasonics, Proceedings of the SPIE smart materials and structures conference, 8-12 March 2009, San Diego, California.